Conformational effects of Lys191 in the human GnRH receptor: mutagenesis and molecular dynamics simulations studies

Eduardo Jardón-Valadez[1,2,*], Arturo Aguilar-Rojas[1,*], Guadalupe Maya-Núñez[1], Alfredo Leaños-Miranda[1], Ángel Piñeiro[2,3], P Michael Conn[1,4] and **Alfredo Ulloa-Aguirre[1,4]**

[1]Research Unit in Reproductive Medicine, Hospital de Ginecobstetricia 'Luis Castelazo Ayala', Instituto Mexicano del Seguro Social, Apartado Postal 99-065, Unidad Independencia, Mexico D.F. CP 10101, Mexico

[2]Departamento de Fisicoquímica, Facultad de Química, Universidad Nacional Autónoma de México, C.U., México D.F. CP04510, Mexico

[3]Departamento de Física Aplicada, Facultad de Física, Universidad de Santiago de Compostela, E-15782 Santiago de Compostela, Spain

[4]Oregon National Primate Research Center, Beaverton, 97006 Oregon, USA

(Correspondence should be addressed to A Ulloa-Aguirre; Email: aulloaa@servidor.unam.mx)

*(E Jardón-Valadez and A Aguilar-Rojas contributed equally to this work)

Abstract

In the present study, we analyzed the role of Lys191 on function, structure, and dynamic behavior of the human GnRH receptor (hGnRHR) and the formation of the Cys14–Cys200 bridge, which is essential for receptor trafficking to the plasma membrane. Several mutants were studied; mutants lacked either the Cys14–Cys200 bridge, Lys191 or both. The markedly reduced expression and function of a Cys14Ser mutant lacking the 14–200 bridge, was nearly restored to wild-type/ΔLys191 levels upon deletion of Lys191. Lys191 removal resulted in changes in the dynamic behavior of the mutants as disclosed by molecular dynamics simulations: the distance between the sulfur- (or oxygen-) sulfur groups of Cys (or Ser)14 and Cys200 was shorter and more constant, and the conformation of the NH_2-terminus and the exoloop 2 exhibited fewer fluctuations than when Lys191 was present. These data provide novel information on the role of Lys191 in defining an optimal configuration for the hGnRHR intracellular trafficking and function.

Journal of Endocrinology (2009) **201,** 297–307

Introduction

The mammalian GnRH receptor (GnRHR) type I (hereafter referred as GnRHR) belongs to the superfamily of G-protein coupled receptors (GPCRs), specifically, to the family related to the rhodopsin- and β_2-adrenergic-like receptors (Family A; Ulloa-Aguirre & Conn 1998, Millar *et al.* 2004). The GnRHR is located in the pituitary gonadotroph and is bathed by the circulation of the hypothalamic–pituitary portal system which transfers pulsatile signals of the hypothalamic decapeptide, GnRH. The gonadotroph cell responds with a concomitant pulsatile release of the gonadotrophins, LH and FSH (Santen & Bardin 1973, Knobil 1974). These enter the peripheral circulation and regulate gonadal steroidogenesis, along with gametogenesis.

The GnRHR is among the smallest members of the GPCR superfamily (328 amino acid residues in the human GnRHR (hGnRHR)); unlike other members of the rhodopsin/β-adrenergic subfamily of GPCR, including the type II GnRHR (Millar 2003), the GnRHR exhibits several unique features such as the reciprocal change of the conserved Asp and Asn residues in transmembrane domains (TM) 2 and 7 (Awara *et al.* 1996), the replacement of Tyr with Ser in the highly conserved Asp-Arg-Tyr (DRY) motif located in the junction of the TM3 and the intracellular loop (IL) 2, and the lack of the carboxyl-terminal extension into the cytosol (McArdle *et al.* 1999, Millar 2003, Millar *et al.* 2004), whose presence is associated with differential physiological receptor regulation (Heding *et al.* 1998, Lin *et al.* 1998). Another important feature of the GnRHR is the amino acid residue at position 191 in the extracellular loop (EL) 2, which is frequently Glu or Gly in many mammals, but is replaced with Lys in primates (Janovick *et al.* 2006, Ulloa-Aguirre *et al.* 2006); in rat and mice GnRHR (327 amino acid residues) this amino acid is absent, conferring the GnRHR increased cell surface membrane expression for agonist (Arora *et al.* 1999). Knowledge of the structural requirements that govern GnRHR intracellular trafficking and cell surface membrane expression is of prime importance considering that this receptor is presently a therapeutic target for a number of pathological conditions such as prostate cancer, uterine fibroids, endometriosis, and precocious puberty.

The amino acid sequence of the hGnRHR predicts formation of two disulfide bridges at extracellular regions, one connecting the first and second ELs (Cys114–Cys196) and the second connecting the amino terminal extension

DOI: 10.1677/JOE-08-0527
0022–0795/09/0201–297
Online version via http://www.endocrinology-journals.org

with the EL2 (Cys14–Cys200; Millar *et al.* 2004). The first bridge that involves two highly conserved cysteine residues is a structural feature present in many GPCRs and it is associated with the fundamental stability of the seven transmembrane structure (Ulloa-Aguirre & Conn 1998). The functional significance of the Cys14–Cys200 bridge differs depending on the receptor species (Knollman *et al.* 2005). In the rat, this bridge is not essential for optimal function of the GnRHR as replacement of the Cys residues at either end of the bridge does not affect plasma membrane expression and agonist-stimulated intracellular signaling (Cook & Eidne 1997, Janovick *et al.* 2002), whereas in the mouse GnRHR, breakage of this bridge results in ~50% decrease in receptor function (Knollman *et al.* 2005). In the human receptor, formation of this bridge is an absolute requirement for efficient routing and plasma membrane expression of the receptor as bridge-breaking mutants Cys200Tyr (a naturally occurring mutation in humans; Beranova *et al.* 2001), Cys14Ala and Cys200Ala (Janovick *et al.* 2002) exhibit either none or marginal activity; further, exposure to these mutants to pharmacological chaperones (i.e., small molecules that serve as molecular scaffolding to promote correct folding of otherwise misfolded mutant proteins), normalize receptor function indicating that the absence of the bridge resulted in a misfolded protein (Leanos-Miranda *et al.* 2002, Knollman *et al.* 2005).

The structural determinants that lead to the requirement of the Cys14–Cys200 bridge in folding and plasma membrane expression of the hGnRHR have been defined by mutagenesis experiments (Janovick *et al.* 2006, 2007). These studies revealed that residues located in the NH_2-terminus and in the EL2 as well as sequences flanking this loop (i.e., within TMs 4 and 5) and those that abut on that area (ELs 1 and 3), presumably control the destabilizing role of Lys191 on the formation of the Cys14–Cys200 bridge. In fact, removal of Lys191 from misfolded hGnRHR mutants (including Cys14Ala and Cys200Tyr mutants) led to partial or complete functional recovery of the altered receptors indicating that the association Cys14–Cys200 may be potentially disrupted or diminished by the presence of Lys191, which is present in primate GnRHRs and absent in mice and rat receptors (Leanos-Miranda *et al.* 2002, Janovick *et al.* 2006).

In the present study, we applied a combined strategy (mutagenesis and functional studies as well as computational modeling and molecular dynamics (MD) simulations) to analyze the role of Lys191 on the functional, structural, and dynamic behavior of the hGnRHR. A model of the wild-type (Wt) hGnRHR in explicit dipalmitoyl phosphatidyl choline bilayers, recently developed in our laboratory and further refined by intensive MD simulations (Jardon-Valadez *et al.* 2008), was employed as reference structure for the mutations and structural modifications. Both experimental and theoretical results provide new insights at the atomic level into this issue, and indicate that the absence of Lys191 favors the interactions between the EL2 and the NH_2-teminus, the formation of the Cys14–Cys200 disulfide bridge, and the acquisition of a hGnRHR configuration compatible with high-plasma membrane expression and function, even in the absence of the Cys14–Cys200 bridge.

Materials and Methods

Construction of hGnRHR mutants

A hGnRHR lacking the apparent disulfide bridge at positions 14 and 200 was constructed by replacing Cys at position 14 of the Wt receptor with Ser as previously reported (Davidson *et al.* 1997). Construction of the hGnRHR Cys14Ser mutant was performed employing the full-length Wt hGnRHR cloned into pcDNA3.1 at *Kpn*I and *Xba*I restriction enzyme sites. Site-directed mutagenesis was performed using the Quick Change site-directed mutagenesis kit (Stratagene, La Jolla, CA, USA), following the manufacturer instructions. Mutagenic oligonucleotides (Life Technologies; forward: 5′-*GAACAGAATCAAAATCACTCTTCAGCCATCAACAACAGC*-3′; reverse: 5′-*GCTGTTGTTGATGGCTGAAGAGTGATTTTGATTCTGTTC*-3′) were designed according to the cDNA sequence reported for the hGnRHR (GenBank accession no. L07949; Chi *et al.* 1993). The hGnRHR Cys14Ser/ΔLys191 mutant was constructed by the above described mutagenesis procedure employing a Wt receptor sequence (cloned in pcDNA3.1) lacking lysine at position 191 (hGnRHR/ΔLys191; Maya-Nunez *et al.* 2002) as template. For transfection, large-scale plasmid DNAs were prepared using an Endofree maxiprep kit (Qiagen). The identity of all constructs was verified by automated sequencing employing the BigDye Terminator Cycle Sequence kit (Applied Biosystems, Foster City, CA, USA).

Transient transfection of COS-7 cells

Wt and mutant hGnRHRs were transiently expressed in COS-7 cells as described (Maya-Nunez *et al.* 2002). Fifty thousand or 1000 cells per well were plated in 48-well plates (for assessing inositol phosphate (IP) production) or 24-well plates (for binding experiments; Costar, Cambridge, MA, USA), respectively, and 20 h later the cells were transfected with 0·050 or 0·2 μg (for IP production or binding studies respectively) hGnRHR DNA constructs per well, using liposome-mediated endocytosis, as described (Leanos-Miranda *et al.* 2005). After transfection, the cells were washed twice with DMEM/0·1% BSA/gentamicin and preloaded with 4 μCi/ml [^{3}H]-myoinositol (for IP assays) or DMEM (for binding studies) as described below. IP production was measured after exposure of the cells to the GnRH agonist, Buserelin (Sigma) for 2 h.

Measurement of IP production

Quantification of IP production by Dowex anion exchange chromatography and liquid scintillation spectroscopy was performed as described previously (Huckle & Conn 1987).

Receptor binding assay

COS-7 cells were transiently transfected as described above. Twenty hours after the start of transfection, the cells were washed twice with warm DMEM/0·1% BSA/10 mM HEPES and cultured in DMEM for 18 h before addition of [^{125}I]-Buserelin (specific activity 700 μCi/μg). Cells were incubated at room temperature for 90 min in the presence or absence of excess (10 μM) unlabelled ligand (Buserelin; Sigma) plus [^{125}I]-Buserelin. Thereafter, the medium was removed, the plates containing the cells were placed on ice, washed twice with ice-cold PBS, and then the cells were solubilized by the addition of 0·2 M NaOH/0·1% SDS. Aliquots of samples were then transferred to glass tubes and counted in a γ-counter (Packard Instruments, Downers Grove, IL, USA). Specific binding was calculated by subtracting non-specific binding (binding measured in the presence of 10 μM Buserelin) from total binding (no GnRH agonist added).

For the radioreceptor assay, COS-7 cells were transfected as described above and incubated at room temperature for 90 min in the presence or absence of excess Buserelin plus [^{125}I]-Buserelin or [^{125}I]-Buserelin plus increasing concentrations (10^{-11} to 10^{-6}) of the unlabelled ligand. Thereafter, the medium was removed and the plates containing the cells were placed on ice and washed twice with ice-cold PBS. The cells were then solubilized by the addition of 0·2 M NaOH/0·1% SDS. Aliquots of samples were then transferred to glass tubes and counted in a γ-counter.

Mutations and structural modifications on the Wt hGnRHR for computational modeling and MD simulations

Five mutations/structural modifications were introduced on a refined hGnRHR model (Jardon-Valadez *et al*. 2008). Mutant hGnRHR Cys14‖200Cys was identical to the original model but with the Cys14–Cys200 disulfide bridge disrupted by reducing both Cys residues. Lysine 191 was deleted in the Wt hGnRHR structure to yield the hGnRHR/ΔLys191 structure. The two previous structural modifications were simultaneously applied to generate the mutant hGnRHR Cys14‖200Cys/ΔLys191. To propose structure–functional relationships with the results obtained from the mutagenesis and biochemical experiments, GnRHR Cys14Ser and hGnRHR Cys14Ser/ΔLys191 mutant computational models were also generated and simulated. Residue substitutions were performed by keeping the backbone atom coordinates of the original structure and replacing the side chains. Rupture of disulfide bridges required the elimination of the corresponding bond restraint from the potential function and the addition of the reducing hydrogen atom in both Cys residues. Deletion of Lys191 was directly performed on the coordinates file of the Wt receptor model, with the peptide bond between Thr190 and Val192 being imposed. In all cases, the steepest descent minimization was performed to prevent unfavorable contacts and highly unstable interactions. Water molecules and lipids present in the original model were preserved in such a manner that only the local environment of the modified EL2 was perturbed. After minimization, a short molecular dynamics relaxation was performed and thereafter three different 35-ns-long MD simulations at 310 K and constant volume were performed for each system. The temperature of the simulations was chosen to reproduce physiological conditions of the protein. Three MD simulations of the refined Wt hGnRHR model (Jardon-Valadez *et al*. 2008) were performed and used as control runs.

Simulation parameters

All systems consisted of 15 449 water molecules, 192 lipid molecules, the mutant receptor structure, and 15 or 14 chlorine ions, depending on the presence or absence of Lys191. Periodic boundary conditions were imposed for a simulation box of $7{\cdot}6\times7{\cdot}6\times13$ nm^3. A total of 18 MD simulations were performed using the GROMACS package (version 3.3.1; Berendsen *et al*. 1995, Lindahl *et al*. 2001, Van Der Spoel *et al*. 2005). The extended simple point charge (SPC/E) water model (Berendsen *et al*. 1987) was used while the 53a6 parameterization of the GROMOS96 force field (Oostenbrink *et al*. 2004) was employed for the protein and the lipid molecules. Water, protein, lipids, and ions were separately coupled to an external temperature bath (using a coupling constant of 0·1 ps) by means of a Berendsen thermostat (Berendsen *et al*. 1984). The long-range interactions were calculated using the efficient Particle Mesh Ewald (Darden *et al*. 1993, Essman *et al*. 1995) with a real space cut-off of 0·9 nm, a 0·12 nm space grid, and a fourth order B-spline interpolation scheme. The equations of motion were integrated using the leap-frog method (Hockney & Eastwood 1988) with a 2 fs time step. The bond lengths and H–O–H angle in water were constrained using the SETTLE algorithm (Miyamoto & Kollman 1992), while the LINCS algorithm (Hess *et al*. 1997) was used to constrain bond lengths in the receptor and lipid molecules. All atom coordinates were stored every 10 ps. The initial velocities of the atoms were randomly assigned to produce a Maxwell distribution corresponding to the temperature at which the simulation will be performed.

Analysis of the trajectories

Root mean square positional deviations (RMSD) of the whole protein backbone, the backbone of the transmembranal domains, and the backbone atoms of the ELs together with those of the NH_2-terminus were calculated throughout the trajectories. Additionally, in order to compare the time evolution of the mutants' trajectories with those of the Wt receptor, RMSD matrices for the α-carbons were calculated. These matrices provide a global comparison of every structure reached along a particular trajectory of a mutant with those sampled for the Wt receptor in a different trajectory. RMS positional fluctuations (RMSF) per residue were also calculated over the last 15 ns of the trajectory. The S–S (or O–S in Cys14Ser mutants) distances between the sulfur

atom of Cys14 (or the oxygen atom of Ser14) and that of Cys200 were determined as a function of time. The blocking average method (Flyvbjerg & Petersen 1989) was used to calculate the S.D. for the S–S distance. Hydrogen bonds between extracellular amino acid residues were also calculated for the trajectories involving the Cys14Ser mutation using a donor–acceptor atom cutoff distance of 3·5 Å and a donor-hydrogen-acceptor angle of $<30°$. All analyses were performed using tools from the GROMACS 3.3.1 package (Berendsen *et al.* 1995, Lindahl *et al.* 2001, Van Der Spoel *et al.* 2005), the viewers RASMOL 2.7 (Sayle & Milnerwhite 1995), VMD 1.8.2 (Humphrey *et al.* 1996), Pymol 0·99 (De Lano 2002), and several computer programs and scripts specifically developed for this purpose.

Statistical analysis

Data from the biochemical studies were analyzed with one-way ANOVA and then with the Walker-Duncan adaptive procedure. Binding parameters were calculated from the dose–response displacement curves using the software GraphPad Prism 4.0 (GraphPad Software Inc., La Jolla, CA, USA).

Results

Functional studies

As shown in Fig. 1A, all hGnRHRs expressed in COS-7 cells specifically bound ^{125}I-Buserelin. In the absence of the Cys14–Cys200 disulfide bridge (hGnRHR Cys14Ser mutant) maximally bound radiolabelled GnRH analog was considerably reduced (at levels 17±2% from that exhibited by the Wt receptor). The binding capability of Wt and mutant hGnRHRs to which Lys191 was removed, markedly increased as compared with their corresponding counterparts bearing this amino acid. Maximal binding of radiolabelled Buserelin to the Cys14Ser/ΔLys191 mutant, however, remained below (at levels 67±8%) that shown by the Wt hGnRHR. The reduced maximal ^{125}I-Buserelin binding of the hGnRHR Cys14Ser/ΔLys191 mutant was apparently due to a decreased relative binding affinity of agonist for this altered receptor (Fig. 1B and Table 1), since the number of functional mutant Cys14Ser/ΔLys191 receptors at the cell surface increased to levels between those of Wt receptor bearing and lacking Lys191.

Despite the markedly reduced analog binding capacity of the hGnRHR lacking the Cys14–Cys200 disulfide bridge this modification did not abolish completely agonist-stimulated activation of the receptor (Fig. 1C and Table 1). Replacement of Cys with Ser at position 14, resulted in ∼50% reduction in maximal IP production in response to saturation concentration of the metabolically stable agonist Buserelin. By contrast, deletion of Lys191 from the Wt and the Cys14Ser mutant receptor provoked a shift of the corresponding IP dose–response curves to the left, yielding comparable ED_{50} values (17·1±4 and 19·1±3 pM for the Wt and mutant hGnRHRs lacking Lys191 respectively) and maximal agonist-stimulated IP production (Table 1).

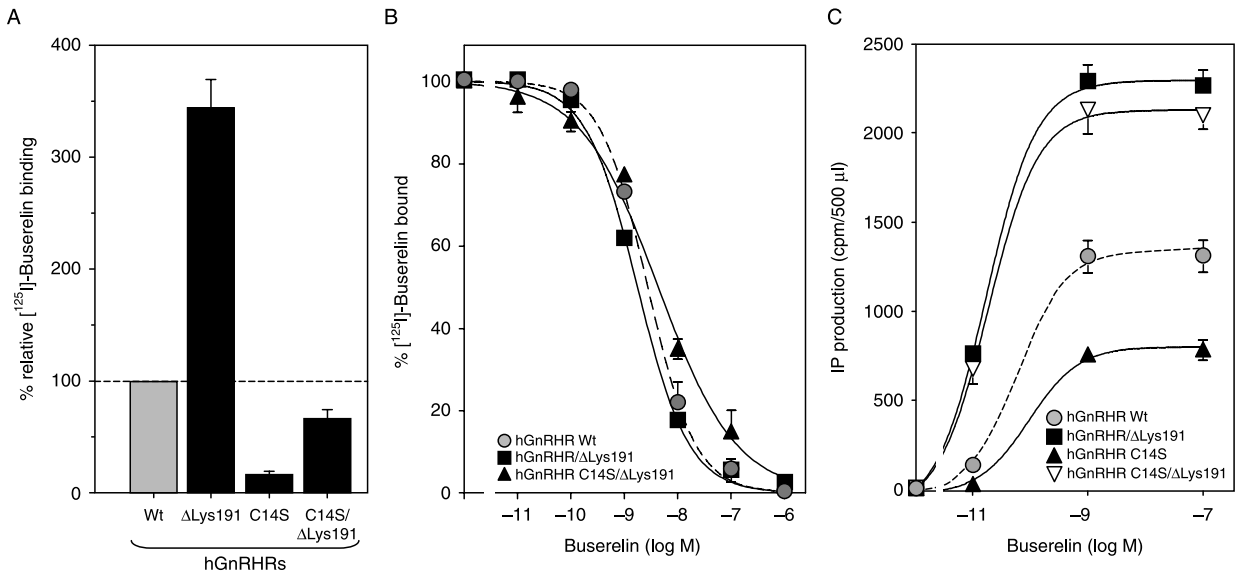

Figure 1 (A) Specific labeled agonist binding to culture COS-7 cells transiently expressing the hGnRHR/ΔLys191, Cys14Ser, and Cys14Ser/ΔLys191 hGnRHRs (black bars). The results are expressed as percentage of [^{125}I]-Buserelin binding relative to that of the Wt hGnRHR (grey bar). (B) Displacement of [^{125}I]-Buserelin by increasing concentrations of unlabelled GnRH agonist in COS-7 cells transfected with the Wt and modified hGnRHRs. (C) Inositol phosphate (IP) dose–response curves for Buserelin in cultured COS-7 cells transiently transfected with the Wt hGnRHR or the hGnRHR/ΔLys191, Cys14Ser or Cys14Ser/ΔLys191 modified hGnRHRs cDNA. The results are the means±S.D. of three independent experiments each carried out in triplicate incubations.

Table 1 Binding parameters, maximal Buserelin-stimulated inositol phosphate (IP) production, and ED_{50} of the wild-type (Wt) and mutant hGnRHRs (means±S.E.M. from three independent experiments)

	GnRH IC_{50} (nM)	**Cell surface receptor** (fmol/10^5 cells)	**Max IP production** (% GnRHR Wt)	**ED_{50}** (pM)
hGnRHR				
hGnRHR Wt	$2{\cdot}4\pm0{\cdot}2^a$	$5{\cdot}5\pm0{\cdot}7^a$	100 ± 4^a	$58{\cdot}9\pm5{\cdot}8^a$
hGnRHR/ΔLys191	$1{\cdot}5\pm0{\cdot}1^b$	$15{\cdot}6\pm1{\cdot}0^b$	174 ± 8^b	$17{\cdot}1\pm0{\cdot}5^b$
hGnRHR Cys14Ser	–	–	60 ± 3^c	$82{\cdot}8\pm3{\cdot}1^c$
hGnRHR Cys14Ser/ΔLys191	$5{\cdot}3\pm0{\cdot}7^c$	$9{\cdot}6\pm0{\cdot}9^b$	162 ± 15^b	$19{\cdot}1\pm2{\cdot}3^b$

Values with different superscript letters within each column are statistically ($P<0{\cdot}05$) different.

In silico *analysis of Wt and mutant hGnRHRs structure*

To assess the role of lysine at position 191 on receptor conformation, three independent trajectories for each mutant generated were monitored by all-atom MD simulations. In all runs, the overall protein structure was well preserved as disclosed by the convergence of the backbone RMSD shown in Figure S1 (see Supplementary data in the online version of the Journal of Endocrinology at http://joe.endocrinology-journals.org/content/vol201/issue2/). RMSD values for the three replicas and the contribution for the helices backbone are also included in the figure. Except for a run in the hGnRHR Cys14‖200Cys mutant, all RMSD values were lower than 3·0 Å throughout the corresponding trajectories. Likewise, the RMSD values for the helices backbone was close to 2·0 Å in all cases. Similar deviations from those configurations sampled in an extended trajectory of the hGnRHR model were detected in all mutant structures (Figure S2, see Supplementary data in the online version of the Journal of Endocrinology at http://joe.endocrinology-journals.org/content/vol201/issue2/). Removal of the Cys14–Cys200 disulfide bridge by reducing both Cys residues (hGnRHR Cys14‖200Cys) or replacing Cys14 by Ser (mutant hGnRHR Cys14Ser) as well as elimination of lysine at position 191 (mutant hGnRHR/ΔLys191) from the Wt receptor resulted in evident conformational changes on the simulated receptor structures. The double mutations involving deletion of Lys191 (mutants hGnRHR Cys14‖200Cys/ΔLys191 and Cys14Ser/ΔLys191) did not present major conformational changes as revealed by their corresponding RMSD values which were comparable with the contributions of the single mutations. In fact, the configuration of hGnRHR Cys14‖200Cys/ΔLys191 would seem to be more similar to the Wt structure than the Cys14‖200Cys receptor (which includes Lys191; Figure S2). As mentioned above, the structural stability of the helice domains suggested that major conformational changes were expected to occur in the extracellular domains (NH_2-terminus and ELs). The RMSDs for the extracellular domains (backbone atoms) and the second EL from one representative run are separately shown in Fig. 2; equivalent plots for the other two runs are included in Figure S3 (see Supplementary data in the online version of the Journal of Endocrinology at http://joe.endocrinology-journals.org/content/vol201/issue2/). Similar time-related profiles were observed for each pair of RMSD, indicating that this analysis was not able to clearly distinguish between different mutants. These plots, together with the RMSD values displayed in Figure S1, also show that the main contribution to the conformational changes of the extracellular domain came from the EL2 and its environment.

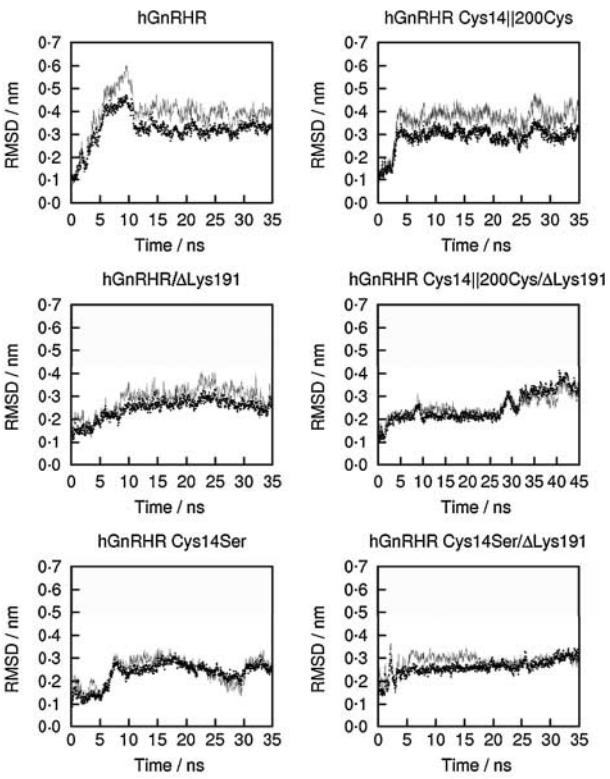

Figure 2 Root mean square positional deviations (RMSD) for the backbone of the extracellular domains (NH_2-terminus and ELs) as a function of time (gray solid lines), and for the backbone of the second extracellular loop (EL2; black dots). Extracellular conformational changes are mostly determined by the EL2 segment.

Figure S4 (see Supplementary data in the online version of the Journal of Endocrinology at http://joe.endocrinology-journals.org/content/vol201/issue2/) shows the RMSFs per residue for the Wt and mutant structures. Residues in the TMs 1–7 were relatively static, while major mobilities were observed in the intra- and ELs, as usually found in other GPCRs (Colson *et al.* 1998). Lysine 191 in the Wt and hGnRHR Cys14‖200Cys structures (or Val192 in hGnRHR/ΔLys191, hGnRHR Cys14‖200Cys/ΔLys191, and hGnRHR Cys14Ser/ΔLys191) is located in the EL2, which is a highly-dynamic domain. In general, maxima and minima RMSF values appeared in the same receptor domains for all mutants and replicas, and although no clear correlations with the presence or absence of Lys191 were detected by this type of analysis, larger fluctuations were observed in those mutants including Lys191 (Figure S4). Nevertheless, differences in Cys14–Cys200 (or Ser14–Cys200) distances were noticed between the hGnRHR Cys14‖200Cys and hGnRHR Cys14‖200Cys/ΔLys191 (or hGnRHR Cys14Ser and hGnRHR Cys14Ser/ΔLys191) structures. Figure 3 and Table 2 show the distance between sulfur atoms of Cys14 and Cys200 for the hGnRHR Cys14‖200Cys and hGnRHR Cys14‖200Cys/ΔLys191 structures as well as that between the oxygen atom of Ser14 and Cys200 for the hGnRHR Cys14Ser and hGnRHR Cys14Ser/ΔLys191 structures as a function of time and for the three replicas of each system. Specifically, in structure hGnRHR Cys14‖200Cys, the S–S distance increased from the initial bond distance to an average of $9{\cdot}85 \pm 0{\cdot}45$ Å in the second run and to $6{\cdot}22 \pm 0{\cdot}11$ Å in the third run. By contrast, in hGnRHR Cys14‖200Cys/ΔLys191 (lacking Lys191) the S–S distance was shorter and more constant in the three replicas even in the absence of the 14–200 disulfide bridge. In the hGnRHR Cys14Ser structure (bearing Lys191), the O–S distance increased up to $7{\cdot}74 \pm 0{\cdot}23$ Å in the first run and was clearly larger in the other two runs than in hGnRHR Cys14‖200Cys/ΔLys191. For the mutant hGnRHR Cys14Ser/ΔLys191, the O–S distance average was $3{\cdot}75 \pm 0{\cdot}08$ Å and $4{\cdot}45 \pm 0{\cdot}10$ Å for the first and second run respectively. Thus, a trend towards more constant and shorter distances between residues at positions 14 and 200 (at the NH_2-terminus and the EL2 respectively) was present in those structures lacking Lys191. The first run of hGnRHR Cys14‖200Cys and the third run in hGnRHR Cys14Ser/ΔLys191 may be considered as borderlines for this trend. Computational limitations did not allow generation of significantly longer trajectories that may clarify whether the corresponding conformations were kinetically trapped. The distances between the residues 14 and 200 of selected final configurations are compared with Wt structure in Fig. 3.

Finally, H-bond networks on hGnRHR Cys14Ser and hGnRHR Cys14Ser/ΔLys191 mutants were analyzed. H-bond pathways involving Ser14, Ser201 (Ser200 when Lys was absent), Ser301 (Ser300), Asp302 (Asp301), and several water molecules around these residues were clearly observed in both receptor structures. These interactions allowed preservation of a serine-rich microdomain even in the absence of the Cys14–Cys200 bridge (Fig. 4A). Interestingly, the formation of those H-bond networks involved less water molecules in the absence of Lys191 (Fig. 4B).

Discussion

As with other GPCRs, a large percentage of the Wt hGnRHR is normally retained in the endoplasmic reticulum and never reaches the cell surface plasma membrane (Ulloa-Aguirre *et al.* 2004, Conn *et al.* 2007). This limited plasma membrane expression of the Wt hGnRH contrasts with that shown by the Wt rat GnRHR, whose cell surface membrane expression exceeds, by more than twofold, that presented by its human counterpart (Janovick *et al.* 2003*b*, 2006). Among the structural differences between these GnRHRs is the presence of Lys191 in the EL2 of the human receptor, which is frequently glutamic acid or glycine in other non-primate mammalian species (Arora *et al.* 1999, Janovick *et al.* 2006, Ulloa-Aguirre *et al.* 2006). Deletion of Lys191 from the hGnRHR or exposure to pharmacological chaperones, markedly increase plasma membrane expression of the Wt receptor to levels comparable with those of the rat GnRHR (Maya-Nunez *et al.* 2002, Janovick *et al.* 2003*a*,*b*, 2006), indicating that the presence of Lys191 limits plasma membrane expression of the human receptor presumably by destabilizing the protein structure (Arora *et al.* 1999). The presence and location of Lys191 in the hGnRHR is of particular interest, since the EL2 is one of the receptor regions showing the largest fluctuations in mobility as indicated by molecular dynamics simulation studies (Jardon-Valadez *et al.* 2008; present study). Although the entire EL2 consists of 27 amino acid residues the presence of two disulfide bonds divides this loop into three distinct segments separated by Cys196 and Cys200. The first segment has five hydrophobic and six polar, non-charged residues as well as Lys191, which exhibits the highest dynamic fluctuations within the EL2 of the receptor (Jardon-Valadez *et al.* 2008).

Mutational and biochemical studies have shown that Lys191 in the hGnRHR destabilizes the association between Cys14 and Cys200, which forms a disulfide bridge that is required for optimal routing of this particular receptor to the cell surface membrane (Janovick *et al.* 2006, Ulloa-Aguirre *et al.* 2006, Conn *et al.* 2007). Apparently, the effect of Lys191 is not wholly an effect of charge because replacement by Ala, Glu, or Gln is also associated with inefficient cell surface membrane expression of the Wt hGnRHR compared with the hGnRHR/ΔLys191 variant (Janovick *et al.* 2006). In fact, replacement of Cys14 or Cys200 with Ala, resulted in almost complete loss of IP production, which was restored to nearly Wt levels by pharmacological chaperones or by deleting Lys191 (Janovick *et al.* 2006), suggesting that the absence of this bridge in the presence of Lys191 yielded a misfolded protein. In the present study, a hGnRHR lacking the apparent disulfide bridge between residues 14 and 200 was constructed by replacing Cys at position 14 of the Wt

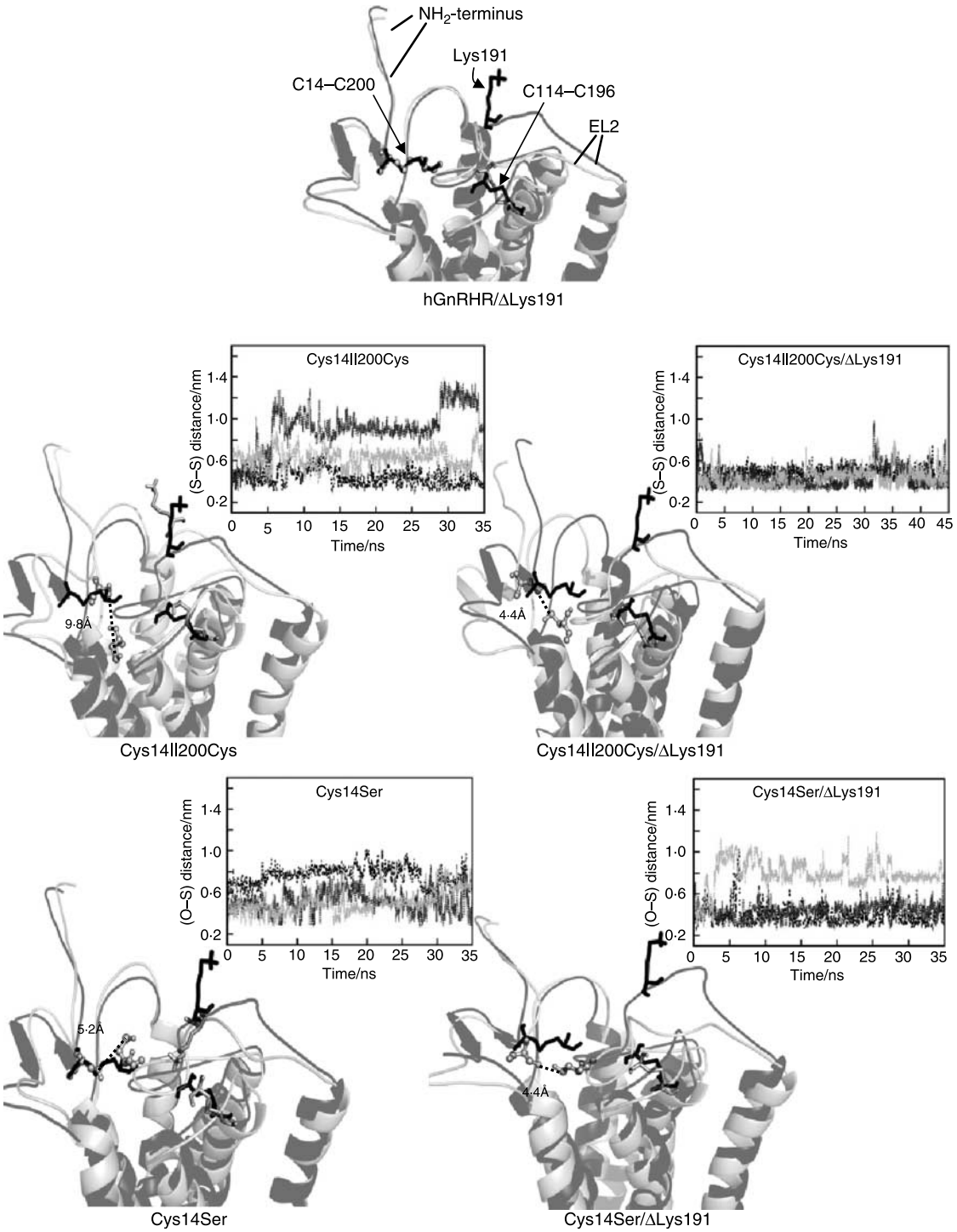

Figure 3 Superposition of the Wt hGnRHR conformation (dark structures) and the final mutant conformations (light structures) in simulation R2. Lysine 191 and the Cys14–Cys200 and Cys114–Cys196 disulfide bridges of the Wt hGnRHR are highlighted in black. Residues C14/S14 and C200 are depicted in balls and sticks. S–S and S–O distances between residues in positions 14 and 200 are also indicated (dotted lines). Insets: distances (in nm) between sulfur and oxygen–sulfur atoms as a function of time for all replicas. Gray scale tones identify the individual simulation runs. Larger average distances and S.D.s are found in mutants bearing Lys191.

Table 2 Average distances between sulfur atoms of Cys14–Cys200 or oxygen and sulfur of Ser14–Cys200 for the last 20 ns of each trajectory

	hGnRHR mutant			
	Cys14‖200Cys S–S distance (Å)	Cys14‖200Cys/ΔLys191 S–S distance (Å)	Cys14Ser O–S distance (Å)	Cys14Ser/ΔLys191 O–S distance (Å)
Run				
1	4·14±0·08	4·74±0·10	7·74±0·23	3·75±0·08
2	9·85±0·45	4·46±0·21	5·24±0·22	4·45±0·10
3	6·22±0·11	4·58±0·07	5·39±0·34	7·89±0·11

S.D. were calculated using the block average method (Flyvbjerg & Petersen 1989). Data were collected during 35 ns (45 ns for Cys14‖200Cys/ΔLys191) for every 10 ps.

receptor with Ser. Despite binding of the GnRH agonist being reduced, the Cys14Ser mutant receptor displayed clearly detectable functional activity (60% of that exhibited by the Wt receptor) but with a rightward shift in the dose–response curve for IP production. These findings are fully consistent with previous data (Davidson *et al.* 1997) and suggest that they more likely resulted from both decreased cell surface membrane expression and low-agonist binding provoked by configurational changes in the NH_2-terminus and also probably in the EL2 (see below). Furthermore, removal of Lys191 from this particular Cys14–Cys200 bridge-lacking mutant completely restored both plasma membrane expression and agonist-stimulated IP production to levels comparable with those exhibited by the Wt receptor lacking Lys191, despite an approximately twofold reduction in binding affinity of the agonist. The fact that removal of Lys191 from the Wt receptor only slightly altered the binding affinity of the receptor for GnRH agonist (Arora *et al.* 1999; present study) and that, in contrast to the Cys14Ser mutant, removal of Lys191 from the Cys14Ala mutant restored receptor function to levels comparable with those of the Wt receptor but well below those achieved by the hGnRHR/ΔLys191 (Janovick *et al.* 2006) strongly suggests that replacement of Cys14 with Ser resulted in gain-of-function of the altered hGnRHR, in which binding affinity was dissociated from receptor activation. In this scenario, removal of Lys191 from the Cys14Ser mutant not only allowed maximal cell surface membrane expression of the receptor but also evidenced the effect of the substitution on the configuration of the receptor and its impact in receptor activation. A similar gain-of-function in receptor activity has been previously detected in a triple mutant hGnRHR with particular substitutions at positions 4, 7, and 10 of the NH_2-terminus (Janovick *et al.* 2006). In the case of the hGnRHR Cys14Ser mutant, our structural analysis suggests that the serine residue was involved in the formation of an extracellular H-bond network (Fig. 4) that, on the one hand, stabilized a particular receptor conformation but, on the other, disturbed binding of agonist due to interactions with Asp302 (Millar *et al.* 2004). This can not be achieved by the Cys14Ala or the Cys14Tyr mutations due to the hydrophobic character of alanine and tyrosine. Although the H-bonds-stabilized conformation could affect the orientation and/or mobility of particular TM helices (e.g., TM1 and/or TM7) such structural changes could not be detected in our limited time-scale MD simulations. Nevertheless, it is conceivable that changes in the configuration of the NH_2-terminus may potentially influence the orientation of the adjacent TM1, and indirectly the intramolecular interactions between Asn53, Asn87 (in TM2), and Asp319 (in TM7) necessary for favoring the equilibrium between the active and inactive conformations of the receptor towards the inactive state (Millar *et al.* 2004). Changes in the conformation of the TM1 may also affect the interaction between Lys36 and Asn102 (Jardon-Valadez *et al.* 2008), the latter involved in GnRH binding (Davidson *et al.* 1996).

Previous mutagenesis studies have documented the functional impact of the differences between the rat GnRHR (no Lys191, high plasma membrane expression) and the hGnRHR (Lys191 present, inefficient plasma membrane expression) sequences and identified those amino acid residues that control the destabilizing influence of Lys191 on the formation of the Cys14–Cys200 disulfide bridge (Knollman *et al.* 2005, Janovick *et al.* 2006). In the present study, we performed MD simulations to analyze the effects of Lys191 on the three-dimensional structure and dynamic behavior of the hGnRHR. For these studies, we departed from a previously refined model of the Wt hGnRHR in an explicit lipid bilayer (Jardon-Valadez *et al.* 2008). All single mutations resulted in configurational changes on the extracellular domains of hGnRHR. Dynamic and structural analysis revealed that the presence of Lys191 provokes a tension between residues at positions 14 and 200, whereas its absence shortens and makes the distance between this pair of residues more stable. Moreover, the distance between Ser14 and Cys200 in the Cys14Ser mutant seemed relatively short and regular (even in the presence of Lys191), probably due to the participation of Ser14 in H-bonds network that may favor receptor stabilization in an active conformation. These results are in line with the assumption derived from mutagenesis studies (Janovick *et al.* 2006, Ulloa-Aguirre *et al.* 2006, Conn *et al.* 2007) regarding the crucial role of Lys191 as well as residues in positions 112, 208, 300, and 302 in determining the final conformation of the EL2 and its association with the

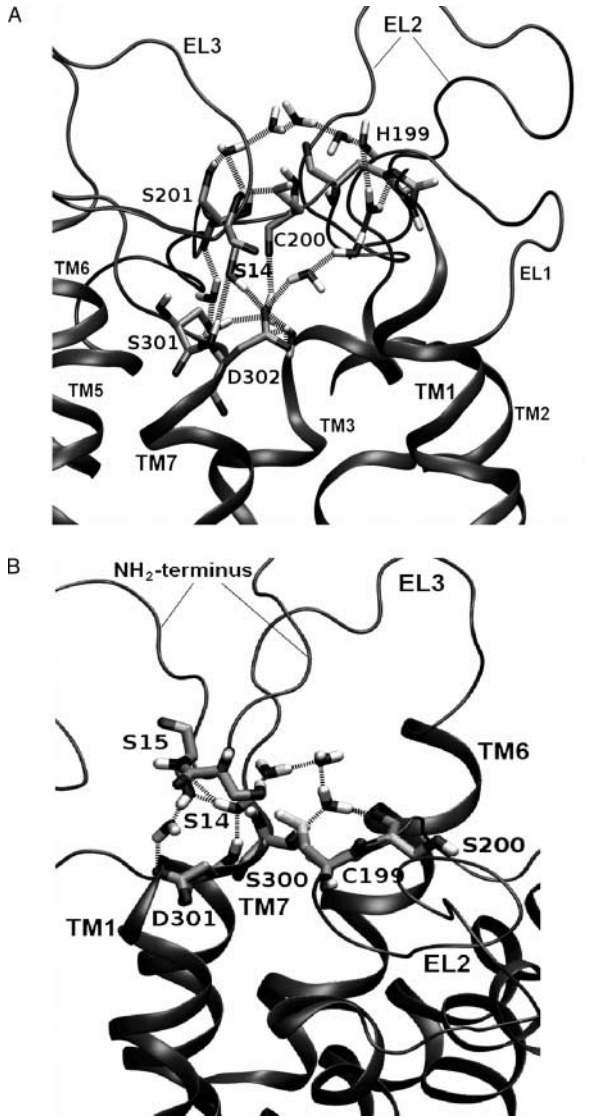

Figure 4 Snapshot showing hydrogen bond networks involving serine at position 14, water molecules, and residues of the ELs 2 and 3 in the presence (A) or absence (B) of Lys191. TM, transmembrane domain; EL, extracellular loop.

NH_2-terminal domain of the receptor. Apparently, the proximity between these two receptor domains represents a fundamental requisite for correct folding and intracellular trafficking of the GnRHR to the plasma membrane. In the Wt rat GnRHR, proximity between the NH_2-terminus and the EL2 is ensured by specific amino acid residues located in several domains, including the TM4, EL2, and TM5, without the need for the formation of the Cys14–Cys199 bridge (Janovick *et al*. 2006), whereas in the Wt hGnRHR (which bears particular amino acids that co-evolved with and presumably control the destabilizing influence of Lys191), the association between these domains needs to be stabilized by the Cys14–Cys200 disulfide bridge, whose rate of formation depends on the proximity between these two cysteine residues (Wedemeyer *et al*. 2000). In this scenario, shorter distances would presumably favor the formation of a stable Cys14–Cys200 disulfide bridge within an efficient time frame during the folding process of the receptor protein thereby reducing its degradation in proteasomes.

In summary, this study provides further evidence of the role of Lys191 in the EL2 of the GnRHR in defining the configuration and the association of this loop with the NH_2-terminus through an interaction between residues in positions 14 and 200, which in the human receptor is mediated by formation of a disulfide bridge. In the absence of Lys191, the cell surface expression of the hGnRHR is enhanced even in the absence of the Cys14–Cys200 bridge. Our findings also offer additional information on the effects of substitutions at Cys14, overemphasizing on the importance of this particular residue in defining the tertiary structure, and function of the hGnRHR.

Declaration of interest

The authors declare that there is no conflict of interest that could be perceived as prejudicing the impartiality of the research reported.

Funding

This study was supported by grants 45991-M (to A U-A) and J49811-Q (to Á-P), from CONACyT, México, grant 2005/1/I/159 from the FOFOI-Instituto Mexicano del Seguro Social, México (to A U-A), grant IN105107 from PAPIIT-UNAM, México (to Á-P), and grants HD-19899, RR-00163, HD-18185, and TW/HD-00668 from the National Institutes of Health, Bethesda, MD, USA (to P M C). Eduardo Jardón-Valadez was a post-doctoral fellow supported by CONACyT, México Eduardo Jardón-Valadez is indebted to the TEMPO group of University of California, Irvine, CA, USA, for providing computing resources.

Acknowledgements

The authors are grateful to the Dirección General de Cómputo Académico (DGSCA) of Universidad Nacional Autónoma de México (UNAM) and to the Centro de Supercomputación de Galicia (CESGA) for computing time and for their excellent service. Ángel Piñeiro thanks Xunta de Galicia for his Isidro Parga Pondal research position. Alfredo Ulloa-Aguirre is recipient of a Research Career Development Award from the Fundación-IMSS, México.

References

Arora KK, Chung HO & Catt KJ 1999 Influence of a species-specific extracellular amino acid on expression and function of the human gonadotropin-releasing hormone receptor. *Molecular Endocrinology* **13** 890–896.

Awara WM, Guo CH & Conn PM 1996 Effects of Asn318 and Asp87Asn318 mutations on signal transduction by the gonadotropin-releasing hormone receptor and receptor regulation. *Endocrinology* **137** 655–662.

Beranova M, Oliveira LM, Bedecarrats GY, Schipani E, Vallejo M, Ammini AC, Quintos JB, Hall JE, Martin KA, Hayes FJ *et al*. 2001 Prevalence,

phenotypic spectrum, and modes of inheritance of gonadotropin-releasing hormone receptor mutations in idiopathic hypogonadotropic hypogonadism. *Journal of Clinical Endocrinology and Metabolism* **86** 1580–1588.

Berendsen HJC, Postma JPM, Van Gunsteren WF, DiNola A & Haak JR 1984 Molecular dynamics with coupling to an external bath. *Journal of Chemical Physics* **81** 3584–3690.

Berendsen HJC, Grigera JR & Straatsma TP 1987 The missing term in effective pair potentials. *Journal of Physical Chemistry* **91** 6269–6271.

Berendsen HJC, van der Spoel LH & van Drunen R 1995 GROMACS: a message-passing parallel molecular dynamics implementation. *Computer Physics Communications* **95** 43–56.

Colson AO, Perlman JH, Smolyar A, Gershengorn MC & Osman R 1998 Static and dynamic roles of extracellular loops in G-protein-coupled receptors: a mechanism for sequential binding of thyrotropin-releasing hormone to its receptor. *Biophysical Journal* **74** 1087–1100.

Conn PM, Ulloa-Aguirre A, Ito J & Janovick JA 2007 G protein-coupled receptor trafficking in health and disease: lessons learned to prepare for therapeutic mutant rescue *in vivo*. *Pharmacological Reviews* **59** 225–250.

Cook JV & Eidne KA 1997 An intramolecular disulfide bond between conserved extracellular cysteines in the gonadotropin-releasing hormone receptor is essential for binding and activation. *Endocrinology* **138** 2800–2806.

Chi L, Zhou W, Prikhozhan A, Flanagan C, Davidson JS, Golembo M, Illing N, Millar RP & Sealfon SC 1993 Cloning and characterization of the human GnRH receptor. *Molecular and Cellular Endocrinology* **91** R1–R6.

Darden T, Darrin Y & Pedersen L 1993 Particle mesh Ewald: an *N*-log(*N*) method for Ewald sums in large systems. *Journal of Chemical Physics* **98** 10089–10092.

Davidson JS, McArdle CA, Davies P, Elario R, Flanagan CA & Millar RP 1996 Asn102 of the gonadotropin-releasing hormone receptor is a critical determinant of potency for agonists containing C-terminal glycinamide. *Journal of Biological Chemistry* **271** 15510–15514.

Davidson JS, Assefa D, Pawson A, Davies P, Hapgood J, Becker I, Flanagan C, Roeske R & Millar R 1997 Irreversible activation of the gonadotropin-releasing hormone receptor by photoaffinity cross-linking: localization of attachment site to Cys residue in N-terminal segment. *Biochemistry* **36** 12881–12889.

Essman U, Perera L, Berkowitz ML, Darden T, Lee H & Pedersen LG 1995 A smooth particle mesh Ewald method. *Journal of Chemical Physics* **103** 8577–8593.

Flyvbjerg H & Petersen HG 1989 Error estimates on averages of correlated data. *Journal of Chemical Physics* **91** 461–466.

Heding A, Vrecl M, Bogerd J, McGregor A, Sellar R, Taylor PL & Eidne KA 1998 Gonadotropin-releasing hormone receptors with intracellular carboxyl-terminal tails undergo acute desensitization of total inositol phosphate production and exhibit accelerated internalization kinetics. *Journal of Biological Chemistry* **273** 11472–11477.

Hess B, Bekker H, Berendsen HJC & Fraaije JGEM 1997 LINCS: a linear constraint solver for molecular simulations. *Journal of Computational Chemistry* **18** 1463–1472.

Hockney RW & Eastwood JW 1988 *Computer Simulation Using Particles*. Bristol, UK: Adam Hilger.

Huckle WR & Conn PM 1987 Use of lithium ion in measurement of stimulated pituitary inositol phospholipid turnover. *Methods in Enzymology* **141** 149–155.

Humphrey W, Dalke A & Schulten K 1996 VMD: visual molecular dynamics. *Journal of Molecular Graphics* **14** 33–38.

Janovick JA, Maya-Nunez G & Conn PM 2002 Rescue of hypogonadotropic hypogonadism-causing and manufactured GnRH receptor mutants by a specific protein-folding template: misrouted proteins as a novel disease etiology and therapeutic target. *Journal of Clinical Endocrinology and Metabolism* **87** 3255–3262.

Janovick JA, Goulet M, Bush E, Greer J, Wettlaufer DG & Conn PM 2003*a* Structure–activity relations of successful pharmacologic chaperones for rescue of naturally occurring and manufactured mutants of the gonadotropin-releasing hormone receptor. *Journal of Pharmacology and Experimental Therapeutics* **305** 608–614.

Janovick JA, Ulloa-Aguirre A & Conn PM 2003*b* Evolved regulation of gonadotropin-releasing hormone receptor cell surface expression. *Endocrine* **22** 317–327.

Janovick JA, Knollman PE, Brothers SP, Ayala-Yanez R, Aziz AS & Conn PM 2006 Regulation of G protein-coupled receptor trafficking by inefficient plasma membrane expression: molecular basis of an evolved strategy. *Journal of Biological Chemistry* **281** 8417–8425.

Janovick JA, Brothers SP, Knollman PE & Conn PM 2007 Specializations of a G-protein-coupled receptor that appear to aid with detection of frequency-modulated signals from its ligand. *FASEB Journal* **21** 384–492.

Jardon-Valadez E, Ulloa-Aguirre A & Pineiro A 2008 Modeling and molecular dynamics simulation of the human gonadotropin-releasing hormone receptor in a lipid bilayer. *Journal of Physical Chemistry* **112** 10704–10713.

Knobil E 1974 On the control of gonadotropin secretion in the rhesus monkey. *Recent Progress in Hormone Research* **30** 1–46.

Knollman PE, Janovick JA, Brothers SP & Conn PM 2005 Parallel regulation of membrane trafficking and dominant-negative effects by misrouted gonadotropin-releasing hormone receptor mutants. *Journal of Biological Chemistry* **280** 24506–24514.

De Lano WL 2002 The PyMOL Molecular Graphics System. In http://www.pymol.org, San Carlos, CA.

Leanos-Miranda A, Janovick JA & Conn PM 2002 Receptor-misrouting: an unexpectedly prevalent and rescuable etiology in gonadotropin-releasing hormone receptor-mediated hypogonadotropic hypogonadism. *Journal of Clinical Endocrinology and Metabolism* **87** 4825–4828.

Leanos-Miranda A, Ulloa-Aguirre A, Janovick JA & Conn PM 2005 *In vitro* coexpression and pharmacological rescue of mutant gonadotropin-releasing hormone receptors causing hypogonadotropic hypogonadism in humans expressing compound heterozygous alleles. *Journal of Clinical Endocrinology and Metabolism* **90** 3001–3008.

Lin X, Janovick JA, Brothers S, Blomenrohr M, Bogerd J & Conn PM 1998 Addition of catfish gonadotropin-releasing hormone (GnRH) receptor intracellular carboxyl-terminal tail to rat GnRH receptor alters receptor expression and regulation. *Molecular Endocrinology* **12** 161–171.

Lindahl E, Hess B & Van Der Spoel D 2001 GROMACS3.0: a package for molecular simulation and trajectory analysis. *Journal of Molecular Modeling* **7** 306–317.

Maya-Nunez G, Janovick JA, Ulloa-Aguirre A, Soderlund D, Conn PM & Mendez JP 2002 Molecular basis of hypogonadotropic hypogonadism: restoration of mutant (E(90)K) GnRH receptor function by a deletion at a distant site. *Journal of Clinical Endocrinology and Metabolism* **87** 2144–2149.

McArdle CA, Davidson JS & Willars GB 1999 The tail of the gonadotrophin-releasing hormone receptor: desensitization at, and distal to, G protein-coupled receptors. *Molecular and Cellular Endocrinology* **151** 129–136.

Millar RP 2003 GnRH II and type II GnRH receptors. *Trends in Endocrinology and Metabolism* **14** 35–43.

Millar RP, Lu ZL, Pawson AJ, Flanagan CA, Morgan K & Maudsley SR 2004 Gonadotropin-releasing hormone receptors. *Endocrine Reviews* **25** 235–275.

Miyamoto S & Kollman PA 1992 SETTLE: an analytical version of the SHAKE and RATTLE algorithms for rigid water models. *Journal of Computational Chemistry* **13** 952–962.

Oostenbrink C, Villa A, Mark AE & van Gunsteren WF 2004 A biomolecular force field based on the free enthalpy of hydration and solvation: the GROMOS force-field parameter sets 53A5 and 53A6. *Journal of Computational Chemistry* **25** 1656–1676.

Santen RJ & Bardin CW 1973 Episodic luteinizing hormone secretion in man. Pulse analysis, clinical interpretation, physiologic mechanisms. *Journal of Clinical Investigation* **52** 2617–2628.

Sayle RA & Milnerwhite EJ 1995 RASMOL: biomolecular graphics for all. *Trends in Biochemical Sciences* **20** 374–376.

Van Der Spoel D, Lindahl E, Hess B, Groenhof G, Mark AE & Berendsen HJ 2005 GROMACS: fast, flexible, and free. *Journal of Computational Chemistry* **26** 1701–1718.

Ulloa-Aguirre A & Conn PM 1998 G protein-coupled receptors and the G protein family. In *Handbook of Physiology. Section 7: The Endocrine System*, pp 87–124. Ed. PM Conn. New York: Oxford University Press.

Ulloa-Aguirre A, Janovick JA, Brothers SP & Conn PM 2004 Pharmacologic rescue of conformationally-defective proteins: implications for the treatment of human disease. *Traffic* **5** 821–837.

Ulloa-Aguirre A, Janovick JA, Miranda AL & Conn PM 2006 G-protein-coupled receptor trafficking: understanding the chemical basis of health and disease. *ACS Chemical Biology* **1** 631–648.

Wedemeyer WJ, Welker E, Narayan M & Scheraga HA 2000 Disulfide bonds and protein folding. *Biochemistry* **39** 7032.

Received in final form 18 February 2009
Accepted 26 February 2009
Made available online as an Accepted Preprint
26 February 2009